Designing Limited Diffraction Beams

Jian-yu Lu, *Member, IEEE*

***Abstract*—Theoretically, limited diffraction beams can only be produced with an infinite aperture. In practice, they can be closely approximated with a finite aperture over a large depth of field. Because of this property, these beams could have applications in medical imaging, tissue characterization, Doppler velocity estimation, and nondestructive evaluation (NDE) of materials, as well as other physics-related areas such as electromagnetics and optics. In this paper, a new method is developed to design limited diffraction beams of desired beam shapes within a finite aperture of interest. It uses previously discovered limited diffraction beams such as Bessel beams and X waves as basis functions, and constructs new beams with linear superpositions of the bases. To construct a new beam of a desired shape, coefficients of the basis functions in the linear superposition are chosen so that the difference between the new beam and a desired beam is minimized under the criterion of least-squares error within the aperture. This procedure is implemented by digitizing both the basis beams and desired beams in the aperture and solving a system of linear equations from its normal equation. The method is applied to several desired beams that are limited diffraction beams known previously. Results show that the designed beams and the desired beams are virtually identical. If the desired beams are not solutions to the wave equation, the designed beams are new limited diffraction beams that are similar in shapes to the desired beams. This suggests that the method may be a powerful and practical tool for developing new limited diffraction beams of desired properties.**

I. Introduction

Limited diffraction beams were first discovered by Stratton in 1941 [1]. These beams were further investigated by Durnin with both computer simulation and optical experiment in 1987 [2],[3]. Durnin termed these beams "nondiffracting beams" or "diffraction-free beams." Because Durnin's terminologies are controversial, we use the new term "limited diffraction beams" [4]. Theoretically, limited diffraction beams can be produced only with an infinite aperture. In practice, they (including other related beams such as "focus wave modes" or "localized waves" discovered first by Brittingham in 1983 [5]) can be closely approximated with a finite aperture over a large depth of field. Because of this property, these beams could have applications in medical imaging [6]–[9], tissue characterization [10], Doppler velocity estimation [11], nondestructive evaluation (NDE) of materials [12], and other physics-related areas such as electromagnetics [13]–[15] and optics [16],[17].

Manuscript received November 30, 1995; accepted June 17, 1996. This work was supported in part by grants CA 54212 and CA 43920 from the National Institutes of Health.

J. Lu is with the Biodynamics Research Unit, Department of Physiology and Biophysics, Mayo Clinic and Foundation, Rochester, MN 55905 (e-mail: jian@mayo.edu).

This work was supported in part by grants CA 54212 and CA 43920 from the National Institutes of Health.

In recent years, limited diffraction beams such as Bessel beams [1]–[3], X waves [18]–[23], bowtie beams [24],[25], and array beams [26] have been studied in detail [27]–[34]. However, a question remains: can an arbitrary beam be represented by a linear superposition of a series of limited diffraction basis beams? The answer is "no." This is because limited diffraction basis beams are solutions to the isotropic/homogeneous wave equation, and their linear combinations are also solutions. Apparently, a desired beam that is not a solution to the wave equation cannot be represeted by such a linear superposition. However, one can always design a limited diffraction beam that is the "closest" to the desired beam within a finite aperture of interest under some criterion. Because desired beams can be arbitrary, numerous limited differaction beams can be developed.

In this paper, a new method to construct limited diffraction beams is developed. In this method, limited diffraction beams discovered previously, such as, Bessel beams [1]–[3] and X waves [18]–[23], are used as basis beams or functions and their linear superpositions are used to represent new limited diffraction beams. To construct limited diffraction beams of desired properties, model beams (desired beams) are used. The "distance" between the constructed (designed) and desired beams is minimized under the criterion of least-squares errors [35] within a finite aperture of interest. With this criterion, coefficients of the basis functions in the linear superpositions can be determined. To implement the method in a computer, both the basis functions and the desired beams are digitized within the finite aperture over a finite axial range. Nyquist sampling rate [36] is satisfied in the digitization. A system of linear equations is derived and its normal equation or the standard singular value decomposition (SVD) [35] is used to solve the unknown coefficients of the basis functions. The solution of the equation automatically satisfies the least-squares criterion. To test the method, several limited diffraction beams known previously are used as desired beams. Results show that the designed beams are virtually identical to these beams. If desired beams are not solutions to the wave equation, the designed beams are new limited diffraction beams that are similar in shapes to these beams. This suggests that the method may be a powerful and practical tool for developing new limited diffraction beams of desired properties.

Hernandez et al. [37] also used the criterion of least-squares error to construct beams. With the Huygen's principle [38], they produced beams that are linear superpositions of spherical waves radiating from point sources. Unlike the method proposed in this paper that uses limted diffraction beams as bases, it is difficult to obtain limited

0885–3010/97$05.00

diffraction beams with their method that uses spherical waves as basis beams.

In this paper, the new method for designing limited diffraction beams is reported in Section II. A few examples are presented in Section III to demonstrate the efficacy of the method. Finally, brief discussion and conclusion are given in Sections IV and V, respectively.

II. Method

There are many ways to develop limited diffraction beams [1],[2],[18],[24] and [28]. In this paper, a new one that uses limited diffraction basis beams (functions) is developed. This method is more practical than the others because it can adapt the properties of designed beams to a desired model beam within a finite aperture of interest. In the following discussion, the Bessel beams and the X waves of various orders are used as basis beams or functions to design monochromatic (single-frequency) and polychromatic (multiple-frequency) limited diffraction beams, respectively.

A. Limited Diffraction Basis Functions

From the isotropic/homogeneous scalar wave equation, one obtains Bessel beams [1],[2] and [18]

$$\begin{aligned}\Phi_{J_n}(\vec{r},t) &= \Phi_{J_n}(r,\phi,z-c_1t)\\ &= J_n(\alpha r)e^{in\phi}e^{i\beta(z-c_1t)}, (n=0,1,2,\dots)\ ,\end{aligned} \quad (1)$$

and X waves [18]

$$\Phi_{X_n}(\vec{r},t) = \Phi_{X_n}(r,\phi,z-c_1t) = e^{in\phi}\int_0^\infty B(k)J_n(kr\sin\zeta)\, e^{-k[a_0-i\cos\zeta(z-c_1t)]}\,dk, (n=0,1,2,\dots)\ , \quad (2)$$

where $\vec{r}=(r,\phi,z)$ represents a spatial point in the cynlindrical coordinates, t is time, r is radial distance, ϕ is polar angle, z is the axial distance, c_1 is the phase velocity (given by $c_1=\omega/\beta$ and $c_1=c/\cos\zeta$ for Bessel beams and X waves, respectively), $\beta=\sqrt{k^2-\alpha^2}>0$ is the propagation constant of Bessel beams, $k=\omega/c$ is the wave number, ω is the angular frequency, c is the speed of sound or light, α is the scaling parameter that determines the mainlobe width of Bessel beams, $\zeta (0\le\zeta<\pi/2)$ is the Axicon angle [39],[40] of X waves, $J_n(\cdot)$ is the nth-order Bessel function of the first kind, $B(k)$ is any well-behaved function that could represent the transfer function of a practical acoustic transducer or electromagnetic antenna, and a_0 is a constant that determines the fall-off speed of the high-frequency components of X waves.

If $B(k)=a_0$, from (2) one obtains the broadband X waves [18]

$$\Phi_{XBB_n}(r,\phi,z-c_1t) = \frac{a_0(r\sin\zeta)^n e^{in\phi}}{\sqrt{M}\left(\tau+\sqrt{M}\right)^n}\ , (n=0,1,2,\dots)\ , \quad (3)$$

where the subscript $_{BB}$ means "broadband" and $M=(r\sin\zeta)^2+\tau^2$, where $\tau=[a_0-i\cos\zeta(z-c_1t)]$.

The above limited diffraction beams are exact solutions to the wave equation. Theoretically, they have an infinite depth of field because the variables z and t appear only in the propagation term, $z-c_1t$, in (1)–(3). In practice, these beams can be closely approximated with a finite aperture over a large depth of field [18]. Assuming that the diameter of the aperture is D, the depth of field of the Bessel beams (1) and the X waves (2) is given by [2],[18]

$$BZ_{\max} = \frac{D}{2}\frac{1}{\sqrt{\left(\frac{c_1}{c}\right)^2-1}} = \frac{D}{2}\sqrt{\left(\frac{k}{\alpha}\right)^2-1} \quad (4)$$

and [18]

$$XZ_{\max} = \frac{D}{2}\frac{1}{\sqrt{\left(\frac{c_1}{c}\right)^2-1}} = \frac{D}{2}\cot\zeta\ , \quad (5)$$

respectively. Notice that the expression, $\frac{D}{2}\frac{1}{\sqrt{(c_1/c)^2-1}}$, is common to both (4) and (5).

B. Designing Limited Diffraction Beams

In the following discussion the limited diffraction basis functions in (1) or (2) will be used to design other limited diffraction beams. Given a desired function, $\Phi_D(\vec{r},t)$, which may or may not be a solution to the wave equation, one can design a limited diffraction beam,

$$\Phi(r,\phi,z-c_1t) = \sum_{n=0}^{\infty} A_n\Phi_n(r,\phi,z-c_1t)\ , \quad (6)$$

that is a linear superposition of the limited diffraction basis functions and is the best approximation to the desired function within the aperture, D, under the criterion of least-squares error [35], where c_1 is a constant (phase velocity) for all basis functions (assume that all the basis beams have the same depth of field (see (4) and (5)), A_n are complex coefficients to be determined, and $\Phi_n(r,\phi,z-c_1t)$ are basis functions in (1) or (2). Because the basis beams in (1) or (2) have the same depth of field, their linear superposition or the new beam (6) has also the same depth of field (see (4) or (5)).

Because (6) is a limited diffraction beam, desired beams should also be of the "limited diffraction" form $\Phi_D(r,\phi,z-c_1t)$, i.e., the variables, z and t, appear only in the propagation term, $z-c_1t$. With such desired beams, the above least-squares problem can be formulated mathematically as follows:

$$\min_{r\le D,\,0\le\phi<2\pi,\text{ and }|z-c_1t|\le d_t} \|\Phi_D(r,\phi,z-c_1t) - \sum_{n=0}^{\infty} A_n\Phi_n(r,\phi,z-c_1t)\|_2\ , \quad (7)$$

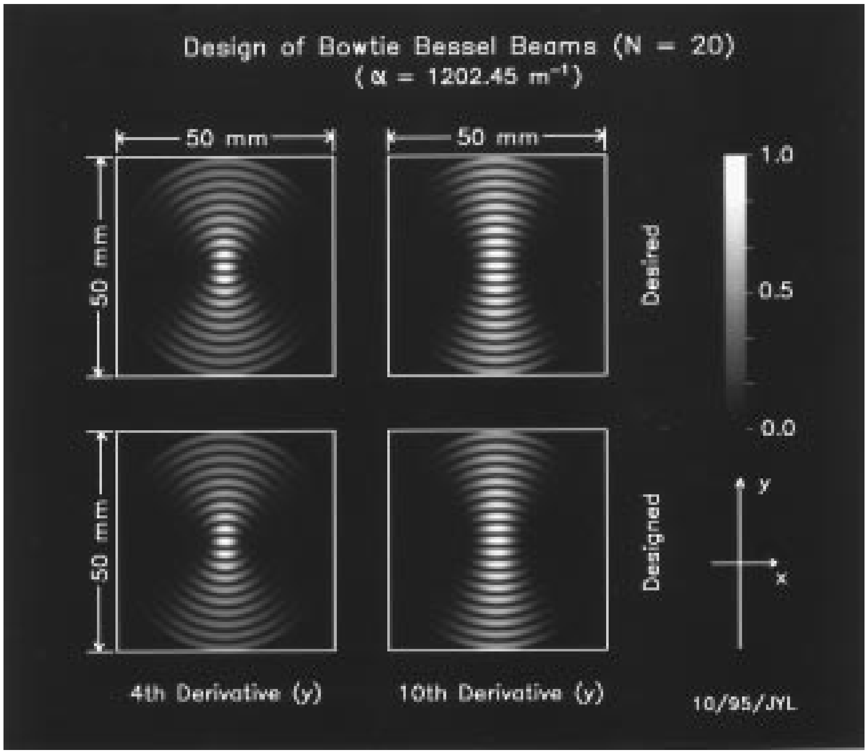

Fig. 1. Design of the 4th (panels in the left column) and the 10th (panels in the right column) derivative bowtie Bessel beams with Bessel basis functions. The desired and the designed beams are in the top and bottom rows, respectively. The absolute values of the transverse components of the beams are shown. The size of each panel is 50 mm × 50 mm, and the scaling parameter, α, for both the bowtie Bessel beams and the Bessel basis functions is 1202.45 m^{-1}. The numbers of terms of the coefficients, D_n and E_n, are N and $N-1$, respectively, where $N = 20$. Notice that the beams are constructed only in a 50 mm diameter area.

where $\|\cdot\|_2$ means L2 norm [35] and d_t represents an axial range beyond which the beams (pulses) have a small amplitude and are negligible. If both the basis beams and the desired beams are monochromatic, the variable z and t can be moved out of (7) and thus the condition, $|z-c_1t| \le d_t$, can be removed. This will be explained later in this section.

C. Matrix Representation

To implement (7) with a system of linear equations of finite number of unknowns, the number of the basis functions in (7) must be truncated. In this case, (7) is given by

$$\min_{r \le D,\, 0 \le \phi < 2\pi,\ \text{and}\ |z-c_1t| \le d_t} \|\Phi_D(r,\phi,z-c_1t) - \sum_{n=0}^{N-1} A_n \Phi_n(r,\phi,z-c_1t)\|_2 \ , \tag{8}$$

where $N \ge 1$ is an integer and is the number of terms of the basis functions. (8) can be solved with the techniques of the linear system of equations and can be written in a matrix form (in the following, the bold fonts represent matrices or vectors) [35]

$$\mathbf{A}\mathbf{x} = \mathbf{b} \ , \tag{9}$$

where

$$\mathbf{A} = [a_{ij}] \ , \tag{10}$$

$a_{ij} = \Phi_j(r^i, \phi^i, z^i - c_1t^i)$ $\{(i = 0, 1, \ldots, M-1), (j = 0, 1, \ldots, N-1)\}$ are the elements of the matrix,

$$\mathbf{x} = \begin{bmatrix} A_0 \\ A_1 \\ \cdots \\ A_{N-1} \end{bmatrix} \tag{11}$$

is a vector variable that contains the unknown coefficients, and

$$\mathbf{b} = \begin{bmatrix} \Phi_D(r^0, \phi^0, z^0 - c_1t^0) \\ \Phi_D(r^1, \phi^1, z^1 - c_1t^1) \\ \cdots \\ \Phi_D(r^{M-1}, \phi^{M-1}, z^{M-1} - c_1t^{M-1}) \end{bmatrix} \tag{12}$$

represents the desired beam vector. The superscript of the variables, r, ϕ, and $z - c_1t$, represents a point in the space and time, and M is the total number of such points (the points are obtained from beams by digitizing within a finite aperture in a finite axial range and the digitization satisfies the Nyquist sampling rate [36]).

From (9), a normal equation can be constructed [35]. If the normal equation has a full rank, N, a solution that satisfies (8) can be obtained [35]

$$\mathbf{x} = (\mathbf{A^T A})^{-1}\mathbf{A^T b} \ , \tag{13}$$

where the superscript, T, means transpose and "−1" represents matrix inversion. If the rank of the matrix, $\mathbf{A^T A}$, is not N, the standard singular value decomposition method [35] can be used to solve (9)

$$\mathbf{x} = \mathbf{V}[\mathrm{diag}(1/\mathrm{w_j})](\mathbf{U^T b}) \ , \tag{14}$$

where $1/w_j$ is replaced with zero if $w_j = 0$, $\mathbf{U}$ is an $M \times N$ column-orthogonal matrix ($M \geq N$), $\mathbf{W} = [w_j]$ is an $N \times N$ diagonal matrix with positive or zero elements, $\mathbf{V}$ is an $N \times N$ orthogonal matrix, and $\mathbf{A} = \mathbf{U}[\mathrm{diag}(\mathrm{w_j})]\mathbf{V^T}$. Solution (14) is also a least-squares solution to (9) or (8) [35]. In addition, it has a minimum norm, min $\|\mathbf{x}\|_\mathbf{2}$ [35].

D. Simplification

Because M in the matrix $\mathbf{A}$ represents the total number of voxels in the volume ($r \leq D, 0 \leq \phi < 2\pi$, and $|z - c_1 t| \leq d_t$), the size of the matrix is usually very large. To reduce the matrix size, in the following we assume that the desired beams are monochromatic and can be expressed in the form

$$\Phi_D(r, \phi, z - c_1 t) = \Phi_{DT}(r, \phi) e^{i\beta(z - c_1 t)} \ , \tag{15}$$

where $c_1 = \omega/\beta$ is a constant, $\Phi_{DT}(r, \phi)$ are the transverse components of the desired beams, and the subscript T means "transverse." In this case, the designed beams can be constructed from the Bessel basis functions (1)

$$\begin{aligned}\Phi(r, \phi, z - c_1 t) &= \sum_{n=0}^{N-1} A_n \Phi_{J_n}(r, \phi, z - c_1 t) \\ &= \left[\sum_{n=0}^{N-1} A_n J_n(\alpha r) e^{in\phi}\right] e^{i\beta(z - c_1 t)} \ .\end{aligned} \tag{16}$$

The assumption in (15) will not lose generality because multiple-frequency limited diffraction beams (pulses) can always be constructed by a linear superposition (or integration) of Bessel beams in terms of frequency [18]. For example, to obtain the X wave basis functions (2), one can integrate the Bessel basis functions (1) over the wave number k with the following parameter substitutions: $\alpha \to k \sin\zeta$ and $\beta \to k \cos\zeta$ [18]. Furthermore, if we assume that $\Phi_{DT}(r, \phi)$ is real, the complex coefficients A_n can be replaced with real coefficients, D_n and E_n, and (16) becomes

$$\begin{aligned}\Phi(r, \phi, z - c_1 t) = [D_0 J_0(\alpha r) &+ \sum_{n=1}^{N-1} D_n J_n(\alpha r) \cos n\phi \\ &+ \sum_{n=1}^{N-1} E_n J_n(\alpha r) \sin n\phi] e^{i(\beta z - \omega t)} \ ,\end{aligned} \tag{17}$$

where we have proved that the new basis functions, $J_n(\alpha r) \left\{ \begin{smallmatrix} \cos n\phi \\ \sin n\phi \end{smallmatrix} \right\} e^{i(\beta z - \omega t)}, (n = 0, 1, 2, \ldots)$, are still exact limited diffraction solutions to the wave equation [33].

From (15) and (17), the matrix and vectors in (9) can be simplified

$$\mathbf{A} = [a_{ij}] \ , \tag{18}$$

$$\mathbf{x} = \begin{bmatrix} D_0 \\ D_1 \\ \cdots \\ D_{N-1} \\ E_1 \\ E_2 \\ \cdots \\ \mathbf{e_{N-1}} \end{bmatrix} , \tag{19}$$

and

$$\mathbf{b} = \begin{bmatrix} \Phi_{DT}(r^0, \phi^0) \\ \Phi_{DT}(r^1, \phi^1) \\ \cdots \\ \Phi_{DT}(r^{M-1}, \phi^{M-1}) \end{bmatrix} , \tag{20}$$

where A is an $M \times (2N - 1)$ matrix, $a_{ij} = J_j(\alpha r^i) \cos j\phi^i$ $\{(i = 0, 1, \ldots, M - 1), (j = 0, 1, \ldots, N - 1)\}$ and $a_{ij} = J_{j-N+1}(\alpha r^i) \sin(j - N + 1)\phi^i$ $\{(i = 0, 1, \ldots, M - 1), (j = N, N + 1, \ldots, 2N - 2)\}$ are the elements of the matrix, $\mathbf{x}$ is a $(2N-1)\times 1$ vector variable, and $\mathbf{b}$ is an $M\times 1$ vector for a desired transverse beam pattern. The solution (13) or (14) with the matrix and vectors in (18)–(20) satisfies the following least-squares formula

$$\begin{aligned}\min_{r \leq D, 0 \leq \phi < 2\pi} \|\Phi_{DT}(r, \phi) - [D_0 J_0(\alpha r) \\ + \sum_{n=1}^{N-1} D_n J_n(\alpha r) \cos n\phi + \sum_{n=1}^{N-1} E_n J_n(\alpha r) \sin n\phi\|_2 \ ,\end{aligned} \tag{21}$$

which does not include the variables z and t. (21) will be the equation for designing the limited diffraction beams in the next section.

III. Results

With (21), one can design limited diffraction beams that are the "closest" to the desired monochromatic beams (15) in a finite aperture of interest. Multiple-frequency limited diffraction beams can then be obtained by an integration over k (see (2)) [18]. Therefore, in the following discussion, only examples for constructions of monochromatic limited diffraction beams will be given.

A. Bowtie Bessel Beams

Bowtie Bessel beams and X waves are limited diffraction beams developed recently (see theory [24], simulations [24], and experiment [25]). These beams were obtained by taking derivatives of (1) and (2), respectively, for $n = 0$ along one transverse direction, say y [24], i.e.,

$$\frac{\partial^m}{\partial y^m} \Phi_{J_o}(r, \phi, z - c_1 t) \tag{22}$$

and

$$\frac{\partial^m}{\partial y^m} \Phi_{X_0}(r, \phi, z - c_1 t) \ , \tag{23}$$

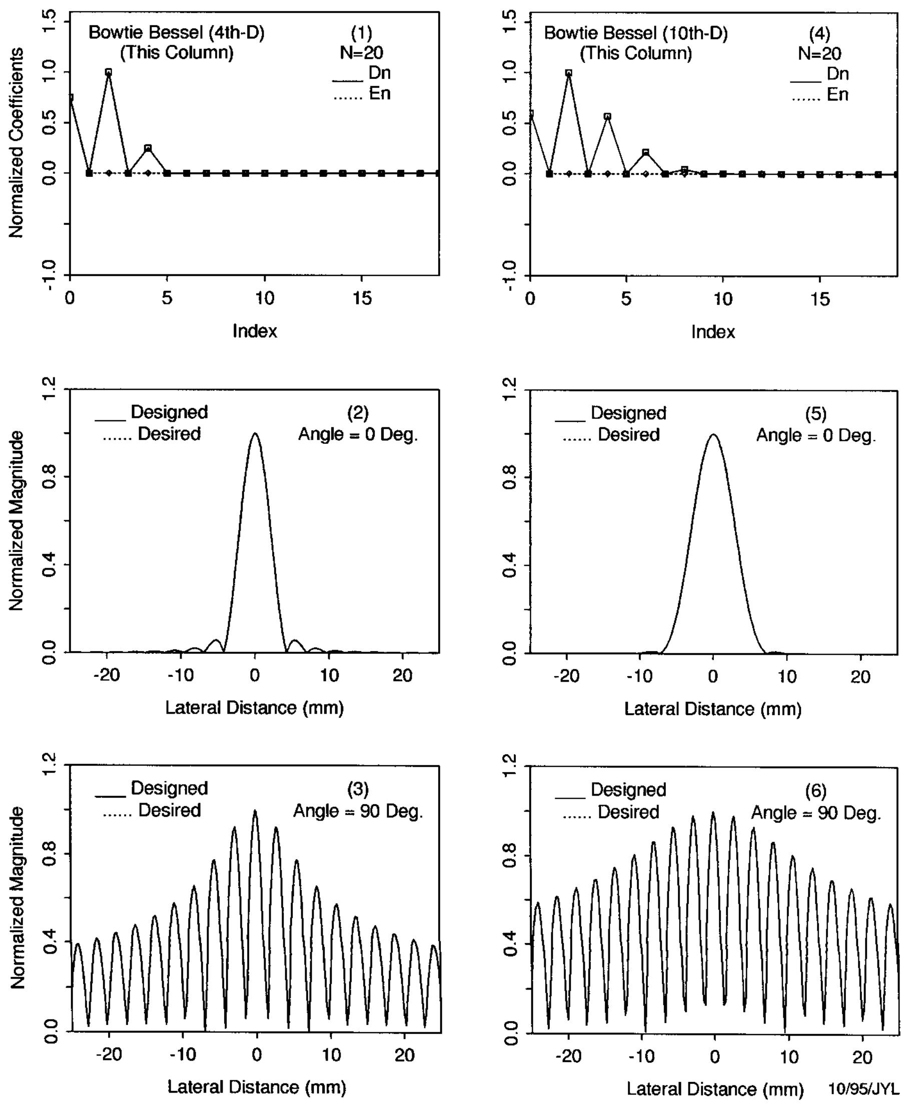

Fig. 2. Line plots of the 4th (panels in the left column) and the 10th (panels in the right column) derivative bowtie Bessel beams in Fig. 1 along the $x(\phi = 0°)$ (panels in the middle row) and the $y(\phi = 90°)$ (panels in the bottom row) axes. The designed and the desired beams are represented by full and dotted lines, respectively. These lines virtually overlap with each other although the number of terms of the Bessel basis functions used in the construction is small ($N = 20$). The coefficients D_n (full lines with square points) and E_n (dotted lines with diamond points) are shown in the panels of the top row. Because D_n and E_n are negligible for $N \geq 9$, the number of terms of the Bessel basis functions can be smaller. The lateral axes of the panels in the bottom two rows are from -25 to 25 mm, and the vertical axes of these panels are normalized to 1.0. The lateral axes of the plots in the top row represent the index, n, and the vertical axes are normalized from -1 to 1.

where m is a nonnegative, even integer. With bowtie beams, sidelobes of pulse-echo systems could be reduced dramatically when these beams are used in transmit and their 90° rotated (around the z axis) responses are used in receive [24].

The absolute values of the bowtie Bessel beams (22) in a transverse plane with $m = 4$ and 10 at $z = c_1 t$ are shown in Fig. 1 in the top panels from left to right, respectively. These beams are called the 4th and 10th derivative bowtie Bessel beams, respectively, and their scaling parameter, α, is 1202.45 m^{-1}. In the following discussion, we assume that this scaling parameter is used for all Bessel basis functions (1) to design limited diffraction beams. In this case, the depth of field of designed beams will be about 216 mm (see (4) and (5)) for a 50 mm diameter aperture and a central frequency of 2.5 MHz. The absolute values of the bowtie X waves in (23) are shown in Fig. 1 of [24].

When the 4th and 10th derivative bowtie Bessel beams are used as desired beams, limited diffraction beams designed with the least-squares formula (21) are virtually identical to the desired beams (see the panels in the bottom row of Fig. 1), although the number of terms of the Bessel basis functions (1) is small ($N = 20$). To show the details of the desired and designed beams, line plots along two axes, $x(\phi = 0°)$ and $y(\phi = 90°)$, of these beams are shown in Fig. 2. The coefficients D_n and E_n (normalized to their maxima), used to construct the beams in (21), are also shown. In fact, if m = 10, (22) is given by:

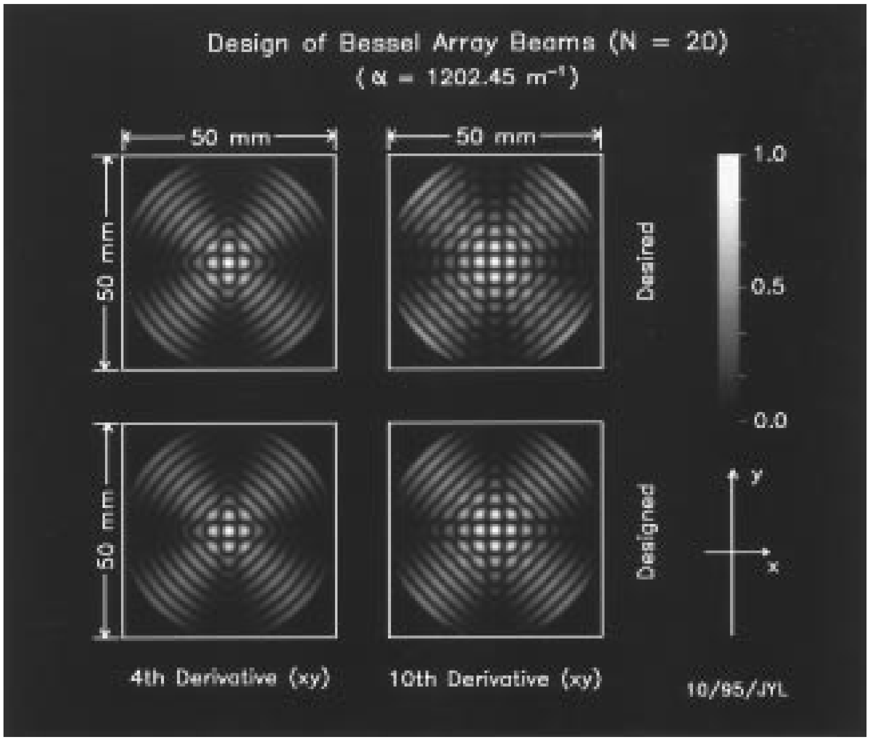

Fig. 3. This figure has the same format as Fig. 1 except that it is for the design of the 4th (panels in the left column) and 10th (panels in the right column) derivative Bessel array beams with Bessel basis functions. The parameters, α and N are also the same as those of the beams in Fig. 1.

$-\alpha^{10}[126J_0(\alpha r) + 210J_2(\alpha r)\cos 2\phi + 120J_4(\alpha r)\cos 4\phi + 45J_6(\alpha r)\cos 6\phi + 10J_8(\alpha r)\cos 8\phi + J_{10}(\alpha r)\cos 10\phi]/512.$

B. Bessel Array Beams

Bessel array beams consist of multiple parallel beams. They were developed recently [26] and could be used for real-time volumetric imaging [41],[42]. This is because when these beams are used in transmit, multiple dynamically focused received beams can be formed simultaneously to increase image frame rate. Bessel array beams were derived by taking derivatives of the zeroth-order Bessel beam (1) along both x and y axes [26]

$$\frac{\partial^{2m}}{\partial x^m y^m}\Phi_{J_0}(r,\phi,z-c_1t) \ , \qquad (24)$$

where m is a nonnegative even integer. These beams are also exact limited diffraction solutions to the wave equation [24],[26].

With $m = 4$ and 10, one obtains the 4th and 10th derivative Bessel array beams, respectively. The absolute values of these beams are shown in the panels of the top row of Fig. 3. Beams designed with (21) are shown in the panels of the bottom row. They are very close to the desired beams in the top row. Line plots of the beams in Fig. 3 along $\phi = 0$ and $45°$ are shown in Fig. 4. The number of terms used in the construction is the same as that of Fig. 1 ($N = 20$).

C. Grid Array Beams

Grid array beams [26] are limited diffraction beams that contain more parallel beams than Bessel array beams. Therefore, they could achieve higher imaging frame rate because more receive beams can be formed simultaneously. These beams were derived from a general limited diffraction solution developed in [18] and they are given by [26]

$$\Phi_G(x,y,z-c_1t) = \cos k_x x \cos k_y y e^{ik_z(z-c_1t)} \ , \qquad (25)$$

where the subscript G represents "grid," k_x and k_y are scaling parameters in the x and y directions, respectively, $k_z = \sqrt{k^2 - k_x^2 - k_y^2} > 0$ is a propagation constant, and $c_1 = c\sqrt{1 + (k_x^2 + k_y^2)/k_z^2} = \omega/k_z$.

The absolute values of a grid array beam with $k_x = k_y = 850.45 \text{ m}^{-1}$ are shown in the left panel of Fig. 5. This beam is used as a desired beam in (9) and (21) for construction. The designed beam is shown in the right panel of Fig. 5. The number of terms of the basis functions ($N = 50$) in the construction is larger than that in the previous examples. Line plots of both the desired and designed beams along two angles, $\phi = 0°$ and $45°$, are shown in Fig. 6 where we see that the two beams are virtually identical. Notice that with the parameters, $k_x = k_y = 850.45 \text{ m}^{-1}$, c_1 in (25) is about the same as that of the Bessel basis beams for the same wave number, k.

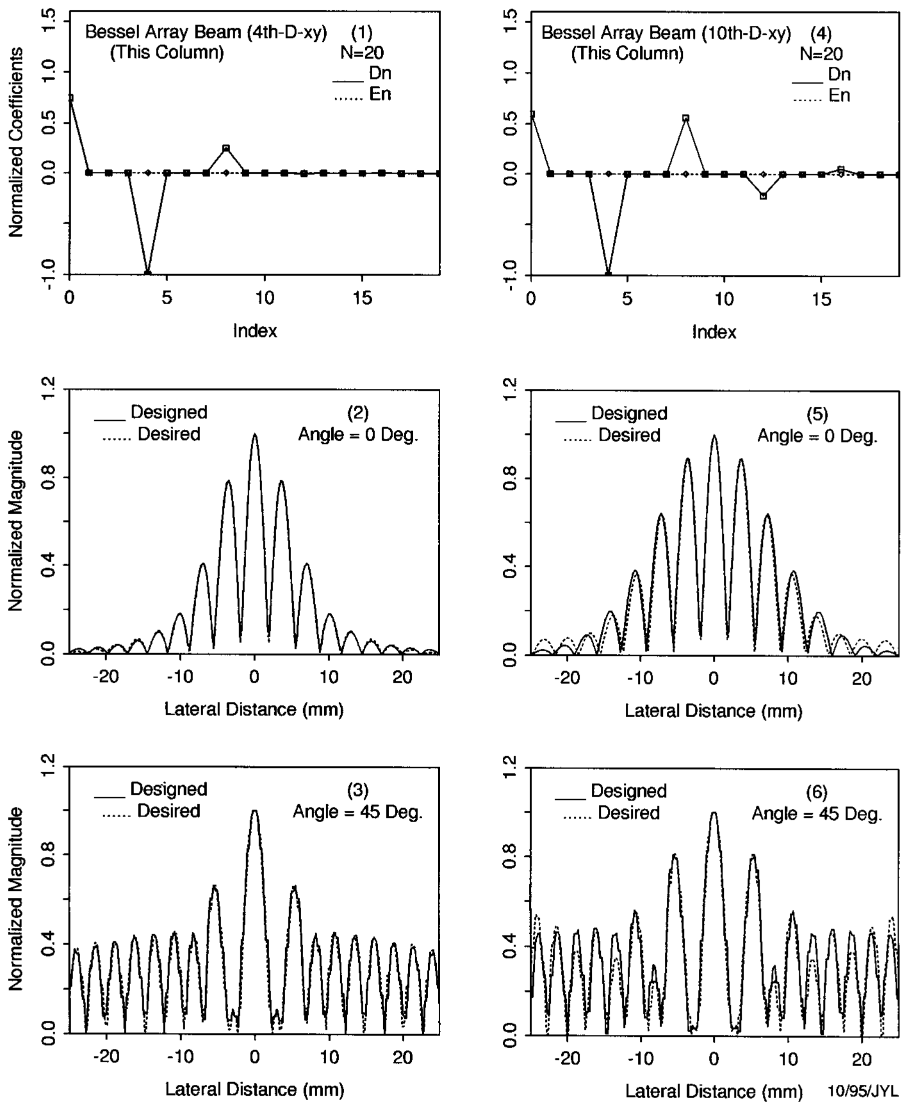

Fig. 4. Line plots of the 4th (panels in the left column) and the 10th (panels in the right column) derivative Bessel array beams in Fig. 3 along the $x(\phi = 0°)$ (panels in the middle row) and the diagonal ($\phi = 45°$) (panels in the bottom row) axes. This figure has the same format as Fig. 2. The non-smoothness of the line plots along the diagonal axis is caused by the nearest-neighbor interpolations from the retangular coordinates.

D. Layered Array Beams

Layered array beams are limited diffraction beams composed of parallel beam layers of equal thickness [26]

$$\Phi_L(x, z - c_1 t) = \cos k_x x e^{ik_z(z - c_1 t)} \ , \qquad (26)$$

where the subscript $_L$ means "layered," k_x is a scaling parameter in the x direction, $k_z = \sqrt{k^2 - k_x^2} > 0$ is a propagation constant, and $c_1 = c\sqrt{1 + k_x^2/k_z^2} = \omega/k_z$.

Layered array beams [26] can be used for the measurement of the transverse component of blood flow velocity [11],[43]. Because the beams have a spatial frequency of k_x in the x direction, the velocity component of blood flow along this direction will cause a spatial modulation of the backscattered signals. The Fourier transform of the signals will produce two peaks on the boundaries of the spectrum. From the distance between the peaks (bandwidth), transverse velocity of blood flow can be determined. This is useful for measuring velocities of blood flow in vessels (such as the carotid artery) that run in parallel with the skin without using a wedge stand. Because of the peaks, the bandwidth of the spectrum can be accurately determined even in a noisy environment and when the beams are not strictly monochromatic and the sampling time is limited. This is an advantage as compared to using a conventional focused piston beam, whose spectrum of the backscattered signals from the focal region has a triangular shape (out of focus, the shape may change) and thus the bandwidth is difficult to determine when there is noise [43]. In addition, because layered array beams are limited diffraction beams, in theory, their spectrum shapes are depth-independent. Application of Bessel beams to the measurement of transverse velocity can also improve the accuracy in a noisy environment because their spectra have shoulders at boundaries. However, the shoulders become smoothed when the beams

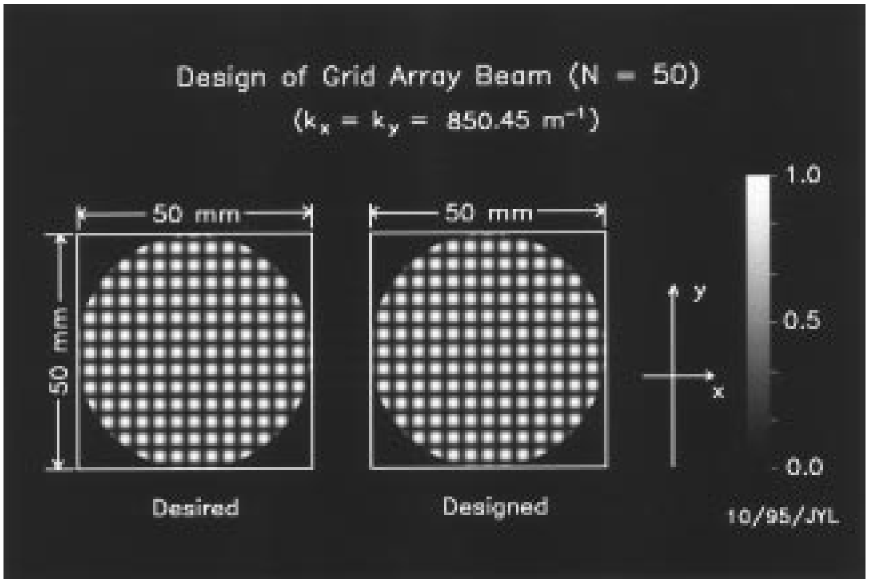

Fig. 5. Design of a grid array beam with Bessel basis functions. The desired beams and the designed beams are on the left and right panels respectively. The absolute values of the transverse components of the beams are shown. The size of each panel is 50 mm × 50 mm. The scaling parameters of the grid array beam are $k_x = k_y = 850.45$ m^{-1}, and the scaling parameter of the Bessel basis functions is 1202.45 m^{-1}. The number of terms of the Bessel basis functions is increased from that in Figs. 1 and 3 ($N = 50$). Notice that the beams are constructed only in a 50 mm diameter area.

are not exactly monochromatic or the sampling time is limited [11].

The absolute values of a layered array beam in (26) are shown in the upper left panel of Fig. 7. To show how to design limited diffraction beams that are the best approximations to the arbitrary designed beams that are not solutions to the wave equation, layered array beams are modified by multiplying the following step

$$u(y) = \begin{cases} 1, & y \geq 0 \\ 0, & \text{Otherwise} \end{cases} \tag{27}$$

and strip

$$p(y) = \begin{cases} 1, & |y| \leq D/12 \\ 0, & \text{Otherwise} \end{cases} \tag{28}$$

functions, where $D = 50$ mm is the diameter of the aperture. The results are shown in the middle and right panels, respectively, of the top row of Fig. 7. Apparently, the modified layer-array beams (also called the step and strip layer-array beams, respectively) are not solutions to the wave equation because any derivative of these beams at the discontinuities within the aperture in the y direction is infinity.

Using the layered array beam and the modified layer-array beams as desired beams, limited diffraction beams that correspond to these beams can be constructed. The results are shown in the panels of the bottom row of Fig. 7, where $N = 50$, $k_x = 1202.45$ m^{-1}, and the scaling parameter of the Bessel basis functions $\alpha = 1202.45$ m^{-1} (with these parameters, $k_z \equiv \beta$). It is seen that for the layered array beam (panels in the left column of Fig. 7), the desired and the designed beams are virtually identical. For layered array beams modified with (27) and (28), the designed beams are similar in shape to the desired beams, but they are not identical. This is because the modified layer-array beams are not limited diffraction solutions to the wave equation, and the designed beams must be. However, the designed beams are the best approximations to the desired beams within the 50 mm diameter aperture, in the sense of the least-squares error defined by (21).

For the desired beams that are the modified layer-array beams, the designed beams are difficult to obtain with methods other than the one developed in this paper. The designed beam corresponding to the layered array beam modified by the step function (27) is very unsymmetrical and is not intuitive to be recognized as a limited diffraction beam having a large depth of field (about 216 mm when produced with a 50 mm diameter and 2.5 MHz central frequency radiator).

Line plots of the layered array beams in Fig. 7 are shown in Fig. 8. The coefficients used in the designs, D_n and E_n, are also shown. Observe that if the desired beam is a step layer-array beam, most of the coefficients $E_n (n = 1, 2, \ldots, N-1)$ of the designed beam (unsymmetrical) are nonzero.

IV. Discussion

A new method for designing limited diffraction beams with the least-squares [35] formulas ((8) or (21)) has been developed. This method uses basis functions that are exact limited diffraction solutions to the isotropic/homogeneous scalar wave equation [18]. The basis functions have been

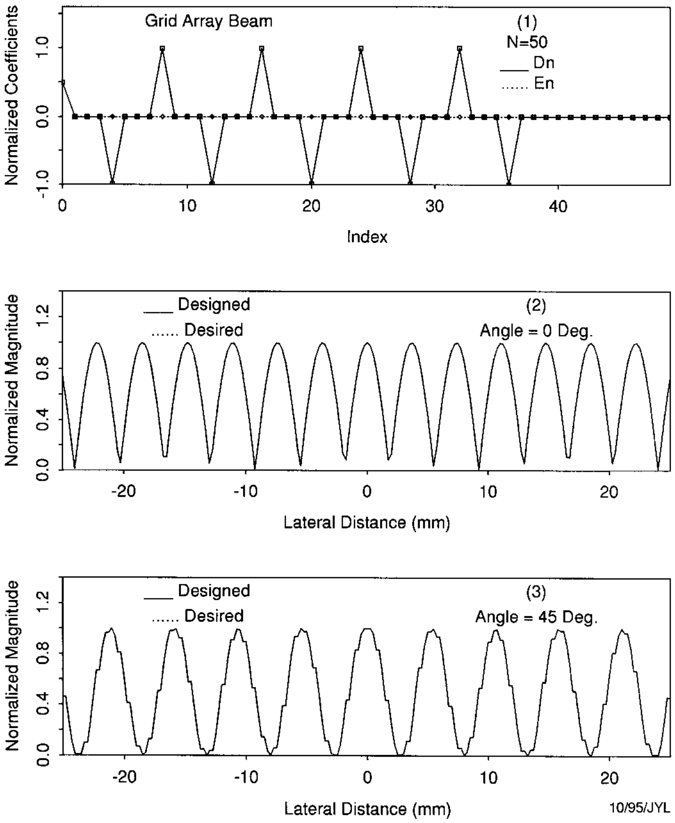

Fig. 6. Line plots of the grid array beams in Fig. 5 along the $x(\phi = 0°)$ (Panel (2)) and the diagonal ($\phi = 45°$) (Panel (3)) axes. This figure has the same format as either the left or right column of Fig. 2. The reason for the non-smoothness of the curves in Panel (3) is the same as that in Fig. 4.

studied extensively in both theory and experiment in the past few years and their properties are well understood [4],[18],[19], and [33]. With the method, a number of newly developed limited diffraction beams such as bowtie Bessel beams [24],[25], Bessel array beams [26], grid array beams [26], and layered array beams [26] are constructed. Even if the desired beams are not solutions to the wave equation, the constructed limited diffraction beams are similar in shapes to the desired beams. Below, we briefly discuss the properties of the new method.

A. Resolution

The lateral resolution of designed limited diffraction beams is determined by that of the basis beams (assume that the scaling parameter α or ζ is the same for all basis beams). To obtain a good construction, the lateral resolutions of designed beams and desired beams should be adjusted to match with each other. For the examples given in the last section, the resolution of the desired beam is matched to that of the designed beam by choosing proper parameters, such as k_x, k_y, and α.

If the scaling parameters are different for the basis beams, designed beams are no longer limited diffraction beams. For example, a linear combination of two Bessel beams of the scaling parameters of α_1 and α_2, respectively, will be a self-constructing beam that reappears at axial distances that satisfy the condition, $\beta_1(z - c_1 t) = (\beta_2(z - c_2 t) \pm 2n\pi$, where n is an integer, and $\beta_1 = \sqrt{k^2 - \alpha_1^2}$ and $\beta_2 = \sqrt{k^2 - \alpha_2^2}$ are propagation constants. In this case, the highest lateral resolution of designed beams is determined by the basis beam that has the largest scaling parameter. Notice that at the distances where the beams repeat their patterns at $z = 0$, sidelobes of the designed beams may be lower than those of the individual basis beams.

B. Sidelobes

Sometimes, desired beams such as bowtie Bessel beams and X waves [24],[25] may have very low sidelobes in some part of the aperture. In general, to improve constructions of such desired beams, a weighted least-squares formula [44] could be used to emphasize the small differences between the low-sidelobe parts of the designed and desired beams

$$\min \|\mathbf{A}'\mathbf{x} - \mathbf{b}'\|_2 \ , \tag{29}$$

where $\mathbf{A}' = \mathbf{fA}$, and $\mathbf{b}' = \mathbf{fb}$, and where $\mathbf{f} = \{f_j\}$ is an $M \times M$ diagonal weighting matrix.

Although beams of low sidelobes are desirable in medical pulse-echo (B-scan) imaging, beams that have high sidelobes may also be useful. In applications such as real-time volumetric imaging and measurement of transverse blood flow velocity, high-sidelobe beams such as Bessel array beams, grid array beams, and layered array beams could be used [26].

C. Depth of Field

The depth of field of the limited diffraction basis beams in (1) and (2) is given by (4) and (5), respectively. For a given central frequency or wave number k and diameter of aperture D, the depth of field is a function of the phase velocity, c_1.

If the depth of field of all basis beams in (1) or (2) is the same, the designed beams (6) also have the same depth of field. In this case, the depth of field of the designed beams is controllable (this is the case for the examples in the previous section).

If a desired beam has fine structures (high lateral resolution), the parameters of the basis beams should be adjusted to match these structures. This means the scaling parameters of the basis functions are larger, or the depth of field ((4) and (5)) is small. This trade-off between lateral resolution and depth of field is similar to that of conventional focused beams.

D. Number of Terms of Basis Functions

In general, the number of terms, N, of the basis functions should be ∞ as shown in (7). In practice, we are only interested in constructing limited diffraction beams

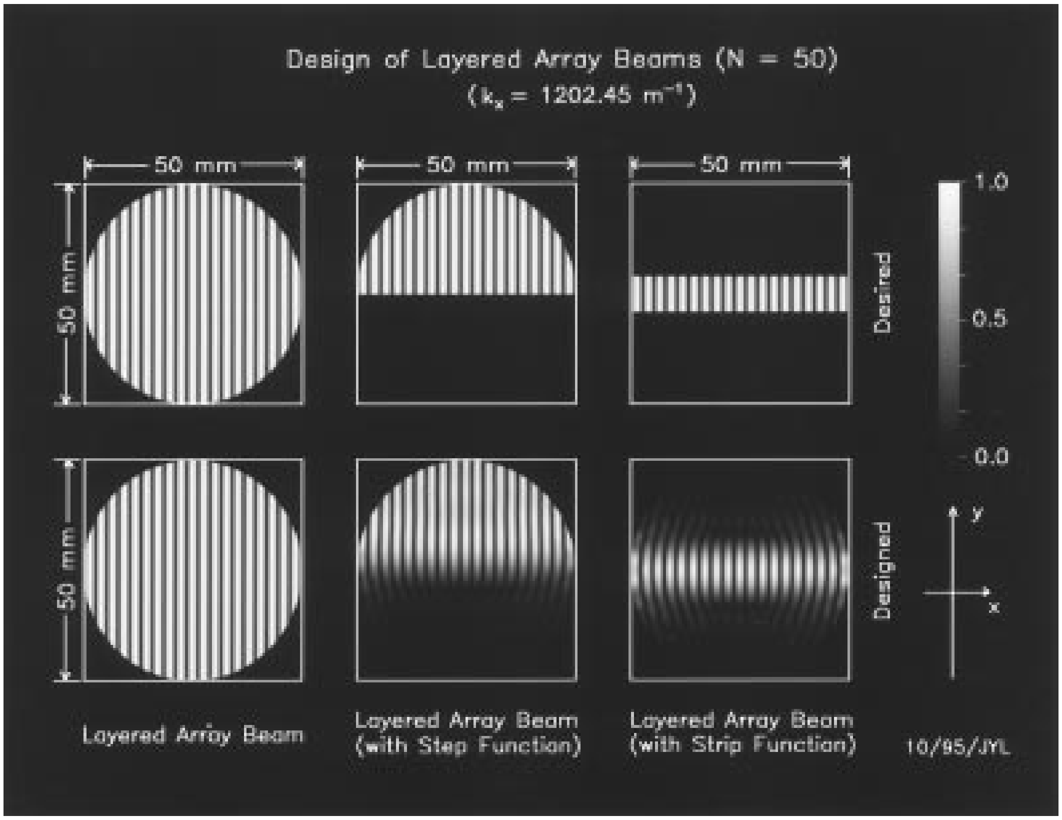

Fig. 7. Line plots of the 4th (panels in the left column) and the 10th (panels in the right column) derivative Bessel array beams in Fig. 3 along the $x(\phi = 0°)$ (panels in the middle row) and the diagonal ($\phi = 45°$) (panels in the bottom row) axes. This figure has the same format as Fig. 2. The non-smoothness of the line plots along the diagonal axis is caused by the nearest-neighbor interpolations from the rectangular coordinates.

in a finite aperture. This means that a finite N is sufficient. This is because as N increases, the order of Bessel functions also increases. Higher-order Bessel functions are close to zero within a finite aperture and thus have little contribution to designed beams.

E. Selection of Desired Beams

In principle, arbitrary beams can be chosen as desired beams. However, one should use the desired beams whose features are the closest to those of the basis beams to obtain a good construction. For example, the desired beams should at least be "limited diffraction" (explicit functions of $z - c_1 t$). If the basis functions are Bessel beams (1), the desired beams should be of the form (monochrome) (15), $\Phi_{DT}(r, \phi)e^{i\beta(z-c_1 t)}$, where c_1 should be the same as that of the Bessel bases. With the modified Bessel basis beams [33] (see (17)), $\Phi_{DT}(r, \phi)$ should be real. One practical way to obtain desired beams would start with limited diffraction beams known previously and then modify from them. Examples were given in the last section where the modified layer-array beams were used as desired beams.

F. Relationship to Basis Beams

If desired beams are limited diffraction beams known previously, the least-squares method developed in this paper actually decomposes these beams into limited diffraction bases. This establishes relationships between the limited diffraction beams and limited diffraction basis beams. In addition, limited diffraction basis beams can be calculated with the Fresnel approximation (see Appendix B of [33]). This simplifies computer simulations of some limited diffraction beams such as the bowtie beams in (22) and (23).

G. Complex Waves

If the transverse component of the desired beams in (15) is complex, the Bessel basis beams in (1) should be used. In this case, beams are constructed with (8) and (9) where the coefficients, $A_n (n = 0, 1, \ldots, N-1)$, are complex.

H. More Beams

Limited diffraction beams of the shape of the step layer-array beam and the strip layer-array beam (Fig. 7) are difficult to obtain by directly solving the wave equation. With the method developed in this paper, we are able to obtain them. Therefore, more limited diffraction beams that might have practical usefulness can be constructed this way. Another advantage of this method is that the designed beams have simple analytic expressions and may be easier to calculate. This is the case for both higher-order bowtie Bessel beams [24] (Fig. 1) and Bessel array beams [26] (Fig. 3).

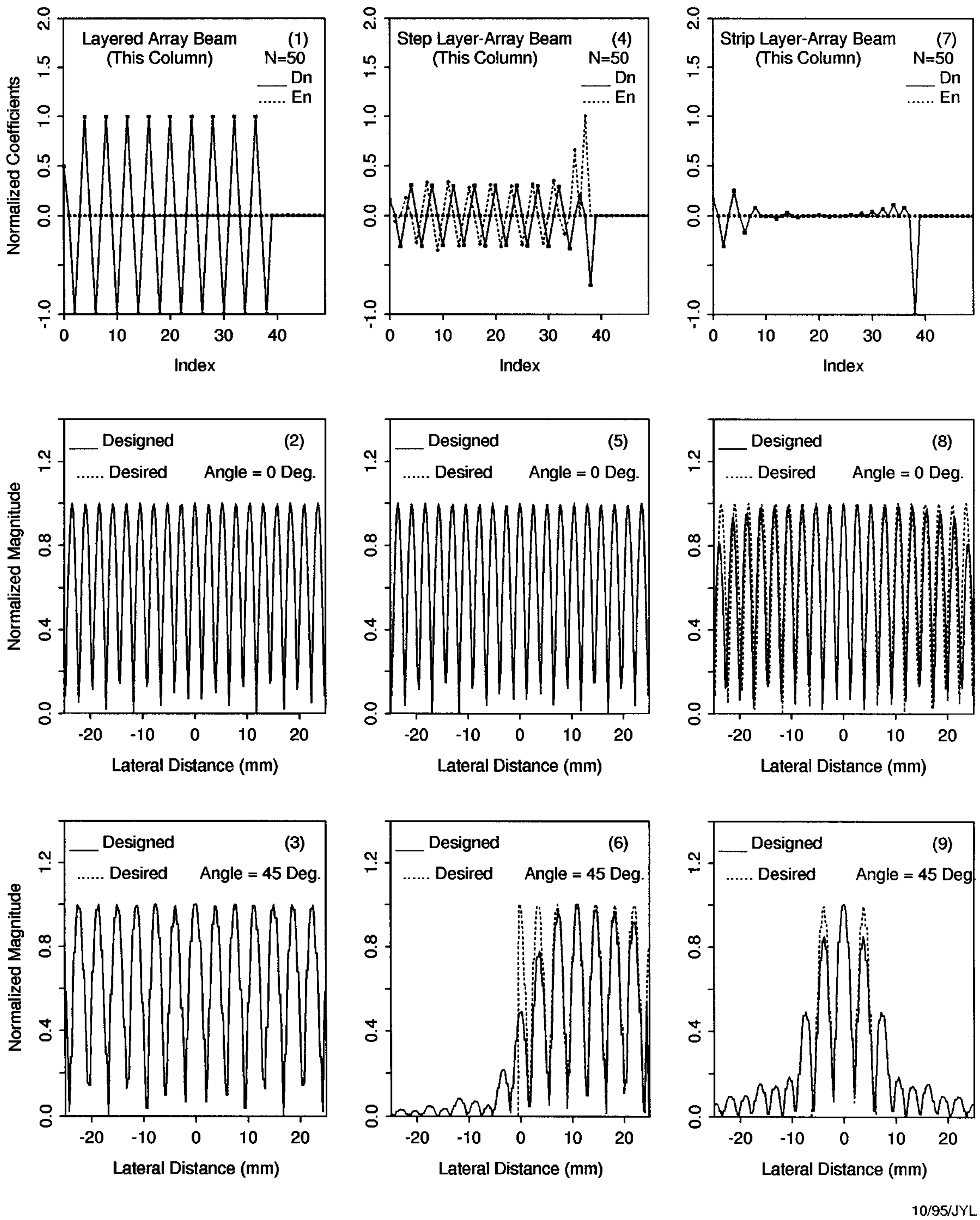

Fig. 8. Line plots of the layered array beams without modification (panels in the left column), modified with a step function (panels in the middle column), and modified with a strip function (panels in the right column) in Fig. 7 along the $x(\phi = 0°)$ (panels in the middle row) and the diagonal ($\phi = 45°$) (panels in the bottom row) axes. This figure has the same format as Fig. 2 except that there is one more column. The reason for the non-smoothness of the curves in the panels of the bottom row is the same as that in Fig. 4.

V. Conclusion

A new method has been developed to design limited diffraction beams that are the closest to desired functions within an aperture of interest in the sense of least-squares error. The method is applied to desired functions that are limited diffraction beams and beams modified from them. The constructed limited diffraction beams are virtually identical to the desired beams when the desired beams are limited diffraction beams. If the desired beams are not limited diffraction beams or not solutions to the wave equation, the designed limited diffraction beams are still similar in shape to the desired beams. This suggests that the method developed in this paper is a robust and powerful tool for obtaining new limited diffraction beams that might have practical usefulness.

Acknowledgments

The author thanks Elaine C. Quarve for secretarial assistance.

References

[1] J. A. Stratton, *Electromagnetic Theory.* New York: McGraw-Hill, p. 356, 1941.

[2] J. Durnin, "Exact solutions for nondiffracting beams. I. The scalar theory," *J. Opt. Soc. Am. A*, vol. 4, no. 4, pp. 651–654, 1987.

[3] J. Durnin, J. J. Miceli, Jr., and J. H. Eberly, "Diffraction-free beams," *Phys. Rev. Lett.*, vol. 58, no. 15, pp. 1499–1501, April 13, 1987.

[4] Jian-yu Lu, He-hong Zou, and J. F. Greenleaf, "Biomedical ultrasound beam forming," *Ultrasound Med. Biol.*, vol. 20, no. 5, pp. 403–428, July 1994.

[5] J. N. Brittingham, "Focus wave modes in homogeneous Maxwell's equations: transverse electric mode," *J. Appl. Phys.*, vol. 54, no. 3, pp. 1179–1189, 1983.

[6] Jian-yu Lu and J. F. Greenleaf, "Diffraction-limited beams and their applications for ultrasonic imaging and tissue characterization," in *New Developments in Ultrasonic Transducers and Transducer Systems*, F. L. Lizzi, Ed., Proceedings SPIE, vol. 1733, pp. 92–119, 1992.

[7] Jian-yu Lu, Tai K. Song, Randall R. Kinnick, and J. F. Greenleaf, "*In vitro* and *in vivo* real-time imaging with ultrasonic limited diffraction beams," *IEEE Trans. Med. Imag.,* vol. 12, no. 4, pp. 819–829, Dec. 1993.

[8] Jian-yu Lu and J. F. Greenleaf, "Pulse-echo imaging using a nondiffracting beam transducer," *Ultrasound Med. Biol.,* vol. 17, no. 3, pp. 265–281, May 1991.

[9] Jian-yu Lu and J. F. Greenleaf, "Ultrasonic nondiffracting transducer for medical imaging," *IEEE Trans. Ultrason., Ferroelect. Freq. Contr.,* vol. 37, no. 5, pp. 438–447, Sept. 1990.

[10] Jian-yu Lu and J. F. Greenleaf, "Evaluation of a nondiffracting transducer for tissue characterization," *IEEE 1990 Ultrason. Symp. Proc.,* 90CH2938–9, vol. 2, pp. 795–798, 1990.

[11] Jian-yu Lu and J. F. Greenleaf, "Application of Bessel beam for Doppler velocity estimation," *IEEE Trans. Ultrason., Ferroelect. Freq. Contr.,* vol. 42, no. 4, pp. 649–662, July 1995.

[12] Jian-yu Lu and J. F. Greenleaf, "Producing deep depth of field and depth-independent resolution in NDE with limited diffraction beams," *Ultrason. Imag.,* vol. 15, no. 2, pp. 134–149, Apr. 1993.

[13] R. Donnelly, D. Power, G. Templeman, and A. Whalen, "Graphic simulation of superluminal acoustic localized wave pulses" *IEEE Trans. Ultrason., Ferroelect., Freq. Contr.,* vol. 41, no. 1, pp. 7–12, 1994.

[14] R. W. Ziolkowski, "Exact solutions of the wave equation with complex source locations," *J. Math. Phys.*, vol. 26, no. 4, pp. 861–863, April 1985.

[15] R. W. Ziolkowski, D. K. Lewis, and B. D. Cook, "Evidence of localized wave transmission," *Phys. Rev. Lett.*, vol. 62, no. 2, pp. 147–150, Jan. 9, 1989.

[16] J. Ojeda-Castaneda and A. Noyola-lglesias, "Nondiffracting wavefields in grin and free-space," *Microwave and Opt. Tech. Lett.,* vol. 3, no. 12, pp. 430–433, Dec. 1990.

[17] G. Indebetow, "Nondiffracting optical fields: Some remarks on their analysis and synthesis," *J. Opt. Soc. Am. A*, vol. 6, no. 1, pp. 150–152, Jan. 1989.

[18] Jian-yu Lu and J. F. Greenleaf, "Nondiffracting X waves—exact solutions to free-space scalar wave equation and their finite aperture realizations," *IEEE Trans. Ultrason., Ferroelect. Freq. Contr.,* vol. 39, no. 1, pp. 19–31, Jan. 1992.

[19] Jian-yu Lu and J. F. Greenleaf, "Experimental verification of nondiffracting X waves," *IEEE Trans. Ultrason., Ferroelect. Freq. Contr.,* vol. 39, no. 3, pp. 441–446, May 1992.

[20] Jian-yu Lu, M. Fatemi, and J. F. Greenleaf, "Pulse-echo imaging with X wave," *Acoust. Imag.,* vol. 22, P. Tortoli, Ed., pp. 191–196, 1996.

[21] M. Fatemi and M. A. Arad, "A novel imaging system based on nondiffracting X waves," *IEEE 1992 Ultrason. Symp. Proc.,* 92CH3118–7, vol. 1, pp. 609–612, 1992.

[22] Tai K. Song, Jian-yu Lu and J. F. Greenleaf, "Modified X waves with improved field properties," *Ultrason. Imag.,* vol. 15, no. 1, pp. 36–47, Jan. 1993.

[23] Jian-yu Lu and J. F. Greenleaf, "Theory and acoustic experiments of nondiffracting X waves," *IEEE 1991 Ultrason. Symp. Proc.,* 91CH3079–1, vol. 2, pp. 1155–1159, 1991.

[24] Jian-yu Lu, "Bowtie limited diffraction beams for low-sidelobe and large depth of field imaging," *IEEE Trans. Ultrason., Ferroelect. Freq. Contr.,* vol. 42, no. 6, pp. 1050–1063, Nov. 1995.

[25] Jian-yu Lu, "Producing bowtie limited diffraction beams with synthetic array experiment," *IEEE Trans. Ultrason., Ferroelect. Freq. Contr.,* vol. 43, no. 5, pp. 893–900, Sept., 1996.

[26] Jian-yu Lu, "Limited diffraction array beams," *Int. J. Imaging Sys. and Tech.*, vol. 8, no. 1, pp. 127–137, Jan., 1997.

[27] D. K. Hsu, F. J. Margetan, and D. O. Thompson, "Bessel beam ultrasonic transducer: Fabrication method and experimental results," *Appl. Phys. Lett.*, vol. 55, no. 20, pp. 2066–2068, Nov. 13, 1989.

[28] Jian-yu Lu, He-hong Zou, and J. F. Greenleaf, "A new approach to obtain limited diffraction beams," *IEEE Trans. Ultrason., Ferroelect. Freq. Contr.,* vol. 42, no. 5, pp. 850–853, Sept. 1995.

[29] Jian-yu Lu and J. F. Greenleaf, "A study of two-dimensional array transducers for limited diffraction beams," *IEEE Trans. Ultrason., Ferroelect. Freq. Contr.,* vol. 41, no. 5, pp. 724–739, Sept. 1994.

[30] J. A. Campbell and S. Soloway, "Generation of a nondiffracting beam with frequency independent beam width," *J. Acoust. Soc. Am.*, vol. 88, no. 5, pp. 2467–2477, Nov. 1990.

[31] Jian-yu Lu and J. F. Greenleaf, "Formation and propagation of limited diffraction beams," in *Acoust. Imag.,* vol. 20, Yu Wei and Ben-li Gu, Ed., pp. 331–343, 1993.

[32] Jian-yu Lu and J. F. Greenleaf, "Comparison of sidelobes of limited diffraction beams and localized waves," *Acoustic Imaging,* vol. 21, Joie Pierce Jones, Ed., pp. 145–152, 1995.

[33] Jian-yu Lu and J. F. Greenleaf, "Sidelobe reduction for limited diffraction pulse-echo systems," *IEEE Trans. Ultrason., Ferroelect. Freq. Contr.,* vol. 40, no. 6, pp. 735–746, Nov. 1993.

[34] Jian-yu Lu and J. F. Greenleaf, "A study of sidelobe reduction for limited diffraction beams," *IEEE 1993 Ultrason. Symp. Proc.,* 93CH3301–9, vol. 2, pp. 1077–1082, 1993.

[35] W. H. Press, B. P. Flannery, S. A. Teukolsky, and W. T. Vetterling, *Numerical Recipes in C.* Cambridge: Cambridge University Press, 1989, chs. 2 and 14.

[36] A. V. Oppenheim and R. W. Schafer, *Digital Signal Processing*, Englewood Cliffs, NJ: Prentice-Hall, 1975, chs. 1 and 5.

[37] J. E. Hernandez, R. W. Ziolkowski, and S. R. Parker, "Synthesis of the driving functions of an array for propagating localized wave energy," *J. Acoust. Soc. Am.,* vol. 92, no. 1, pp. 550–562, July 1992.

[38] J. W. Goodman, *Introduction to Fourier Optics.* New York: McGraw-Hill, 1968, chs. 2–4.

[39] C. B. Burckhardt, H. Hoffmann, and P. A. Grandchamp, "Ultrasound axicon: a device for focusing over a large depth," *J. Acoust. Soc. Am.*, vol. 54, no. 6, pp. 1628–1630, Dec. 1973.

[40] F. S. Foster, M. S. Patterson, M. Arditi, and J. W. Hunt, "The conical scanner: a two transducer ultrasound scatter imaging technique," *Ultrason. Imag.*, vol. 3, no. 1, pp. 62–82, Apr. 1981.

[41] S. W. Smith, H. G. Pavy, Jr., and O. T. von Ramm, "High-speed ultrasound volumetric imaging system—Part I: Transducer design and beam steering," *IEEE Trans. Ultrason., Ferroelect. Freq. Contr.*, vol. 38, No. 2, pp. 100–108, Mar. 1991.

[42] O. T. von Ramm, S. W. Smith, and H. G. Pavy, Jr., "High-speed ultrasound volumetric imaging system—Part II: Parallel processing and image display," *IEEE Trans. Ultrason., Ferroelect. Freq. Contr.*, vol. 38, No. 2, pp. 109–115, Mar. 1991.

[43] V. L. Newhouse, E. S. Furgason, G. F. Johnson, and D. A. Wolf, "The dependence of ultrasound Doppler bandwidth on beam geometry," *IEEE Trans. Sonic. Ultrason.*, vol. SU-27, pp. 50–59, 1980.

[44] G. H. Golub and C. F. Van Loan, *Matrix Computations.* Baltimore, Maryland: The Johns Hopkins University Press, 1988, chs. 6 and 12.

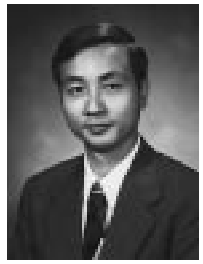

Jian-yu Lu (S'88–M'88) was born in Fuzhou, Fujian Province, People's Republic of China. He received the B.S. in electrical engineering in February, 1982 from Fudan University, Shanghai, China, the M.S. degree in 1985 from Tongji University, Shanghai, China, and Ph.D. degree in 1988 from Southeast University, Nanjing, China. He has been an Assistant Professor of Biophysics at the Mayo Medical School since 1991, and an Associate Consultant at the Biodynamics Research Unit, Department of Physiology and Biophysics, Mayo Clinic, Rochester, MN, since 1992. From March, 1990 to December, 1991 he was a Research Associate at the Biodynamics Research Unit, and from December, 1988 to February, 1990, he was a postdoctoral Research Fellow there. Prior to that, he was a faculty member of the Department of Biomedical Engineering, Southeast University, Nanjing, China and worked with Prof. Yu Wei. His research interests are in acoustic imaging and tissue characterization, medical ultrasonic transducers, and ultrasonic beam forming and propagation. Dr. Lu is a recipient of the Outstanding Paper Award for two papers published in the 1992 IEEE Transactions on the UFFC. He also received the FIRST Award from the NIH, the Biomedical Engineering Research Grant Award from the Whitaker Foundation, and the 1992 Edward C. Kendall Award from Mayo Alumni Association, Mayo Foundation. He is a member of the IEEE UFFC Society, American Institute of Ultrasound in Medicine, and Sigma Xi.